



HAL
open science

Characterization of the Amino Acids Involved in Substrate Specificity of Methionine Sulfoxide Reductase A

Adeline Gand, Mathias Antoine, Sandrine Boschi-Muller, Guy Branlant

► **To cite this version:**

Adeline Gand, Mathias Antoine, Sandrine Boschi-Muller, Guy Branlant. Characterization of the Amino Acids Involved in Substrate Specificity of Methionine Sulfoxide Reductase A. *Journal of Biological Chemistry*, 2007, 282 (28), pp.20484-20491. 10.1074/jbc.M702350200 . hal-01690658

HAL Id: hal-01690658

<https://hal.univ-lorraine.fr/hal-01690658>

Submitted on 23 Jan 2018

HAL is a multi-disciplinary open access archive for the deposit and dissemination of scientific research documents, whether they are published or not. The documents may come from teaching and research institutions in France or abroad, or from public or private research centers.

L'archive ouverte pluridisciplinaire **HAL**, est destinée au dépôt et à la diffusion de documents scientifiques de niveau recherche, publiés ou non, émanant des établissements d'enseignement et de recherche français ou étrangers, des laboratoires publics ou privés.

Characterization of the Amino Acids Involved in Substrate Specificity of Methionine Sulfoxide Reductase A*

Received for publication, March 19, 2007, and in revised form, May 9, 2007 Published, JBC Papers in Press, May 11, 2007, DOI 10.1074/jbc.M702350200

Adeline Gand, Mathias Antoine, Sandrine Boschi-Muller, and Guy Branlant¹

From the Maturation des ARN et Enzymologie Moléculaire, Unité Mixte de Recherche CNRS-UHP 7567, Nancy Université, Faculté des Sciences et Techniques, Bld. des Aiguillettes, BP 239, 54506 Vandoeuvre-les-Nancy, France

Methionine sulfoxide reductases (Msrs) are ubiquitous enzymes that catalyze the thioredoxin-dependent reduction of methionine sulfoxide (MetSO) back to methionine. *In vivo*, Msrs are essential in protecting cells against oxidative damages on proteins and in the virulence of some bacteria. There exists two structurally unrelated classes of Msrs. MsrAs are stereo-specific toward the *S* epimer on the sulfur of the sulfoxide, whereas MsrBs are specific toward the *R* isomer. Both classes of Msrs display a similar catalytic mechanism of sulfoxide reduction by thiols via the sulfenic acid chemistry and a better affinity for protein-bound MetSO than for free MetSO. Recently, the role of the amino acids implicated in the catalysis of the reductase step of *Neisseria meningitidis* MsrA was determined. In the present study, the invariant amino acids potentially involved in substrate binding, *i.e.* Phe-52, Trp-53, Asp-129, His-186, Tyr-189, and Tyr-197, were substituted. The catalytic parameters under steady-state conditions and of the reductase step of the mutated MsrAs were determined and compared with those of the wild type. Altogether, the results support the presence of at least two binding subsites. The first one, whose contribution is major in the efficiency of the reductase step and in which the ϵ -methyl group of MetSO binds, is the hydrophobic pocket formed by Phe-52 and Trp-53, the position of the indole ring being stabilized by interactions with His-186 and Tyr-189. The second subsite composed of Asp-129 and Tyr-197 contributes to the binding of the main chain of the substrate but to a lesser extent.

Methionine is one of the amino acids in proteins that is the most sensitive to reactive oxygen species (1). It is converted into methionine sulfoxide (MetSO),² the function of which is a mixture of two epimers at the sulfur atom, *i.e.* Met-*S*-SO and Met-*R*-SO (2). Formation of MetSO may impair the biological function of the oxidized proteins, depending on the location of the MetSO in the protein. There exist two structurally unrelated

classes of methionine sulfoxide reductases (Msrs) in most organisms, called MsrA and MsrB, which selectively reduce free or protein-bound Met-*S*-SO and Met-*R*-SO, respectively. Msrs are described to exert various biological functions *in vivo* (3–5). They can (i) repair oxidized proteins, and thus, may regulate their function, (ii) play an antioxidant role as oxidation of surface methionine residues is considered as a mechanism that scavenges reactive oxygen species without modification of the properties of proteins, and (iii) play a role in the virulence of some bacteria.

The catalytic mechanism of both classes of Msrs characterized to date (6–9) is composed of three steps including: 1) a reductase step consisting of a nucleophilic attack of the catalytic Cys residue on the sulfur atom of the sulfoxide substrate that leads to formation of a sulfenic acid intermediate and release of 1 mol of Met/mol of enzyme, 2) formation of an intradisulfide bond between the catalytic Cys and a recycling Cys with a concomitant release of 1 mol of water, and 3) reduction of the Msr disulfide bond by thioredoxin (Trx) that leads to regeneration of the reduced form of Msr and to formation of oxidized Trx. The catalytic mechanism is in agreement with the kinetic mechanism, which was shown to be of ping-pong type for both classes of Msrs (9, 10). Moreover, for both classes of Msrs, the overall rate-limiting step is associated with the Trx-recycling process, whereas the rate of formation of the intradisulfide bond is governed by that of the reductase step, the rate of which is fast (11, 12).

A theoretical study of the reduction mechanism of sulfoxides by thiols has been recently investigated by quantum chemistry calculations, which supports formation of a sulfurane intermediate (13). The amino acids involved in the catalysis of the reductase step of *Neisseria meningitidis* MsrA have also recently been characterized by molecular enzymology approaches (14). The invariant Glu-94,³ and to a lesser extent Tyr-82 and Tyr-134, were shown to play a major role in the stabilization of the transition state of sulfurane type and indirectly in the decrease of the pK_{app} of the catalytic Cys-51. A scenario was proposed in which the substrate binds to the active site with its sulfoxide function largely polarized via interactions with Glu-94, Tyr-82, and Tyr-134 and participates via the positive or partially positive charge borne by the sulfur of the sulfoxide to the stabilization of the catalytic Cys.

The three-dimensional structures of the MsrAs from *Escherichia coli*, *Bos taurus*, *Mycobacterium tuberculosis*, and poplar

* This work was supported by grants from the CNRS, the University of Nancy I, the Institut Federatif de Recherche 111 Bioingénierie, the Association pour la Recherche sur le Cancer (ARC Number 5436), and the French Ministry of Research (ACI BCMS047) and by financial support from the French Ministry of Research (to M. A. and A. G.). The costs of publication of this article were defrayed in part by the payment of page charges. This article must therefore be hereby marked "advertisement" in accordance with 18 U.S.C. Section 1734 solely to indicate this fact.

¹ To whom correspondence should be addressed. Tel.: 33-3-83-68-43-04; Fax: 33-3-83-68-43-07; E-mail: Guy.Branlant@maem.uhp-nancy.fr.

² The abbreviations used are: MetSO, methionine sulfoxide; AcMetSONHMe, Ac-L-Met-*R,S*-SO-NHMe; AcMetNHMe, Ac-L-Met-NHMe; Msr, methionine sulfoxide reductase; Trx, thioredoxin.

³ In this report, MsrA amino acid numbering is based on *E. coli* MsrA sequence (9).

have been recently obtained by x-ray crystallography (15–18). The MsrA models describe a single-domain protein composed of a central core around which the long N- and C-terminal coils seem to wind. The overall fold is of the mixed α/β type, with the core containing a two-layer sandwich, α - β plaits motif. The active site can be represented as an opened basin easily accessible to the MetSO substrate in which the catalytic Cys-51 is situated at the entrance of the first α -helix of the central core. In all the structures, the active site is occupied by a molecule that is covalently or noncovalently bound to the Cys-51. In particular, in the *E. coli* MsrA, a dimethyl arsenate is covalently bound, whereas in the *M. tuberculosis* MsrA, a methionine residue (Met-1) from a neighboring monomer occupies the active site. In both cases, a water molecule is present, the position of which can mimic the oxygen atom of the sulfoxide function of the substrate. One of the methyl groups of the dimethyl arsenate and the ϵ -methyl group of Met-1 are bound to a hydrophobic pocket formed by invariant Phe-52 and Trp-53 residues. The Trp-53 indole ring is in interactions with invariant His-186 and Tyr-189 residues, whereas invariant Asp-129 and Tyr-197 residues are in a position to interact with the NH main chain of the Met-1 that occupies the active site of the *M. tuberculosis* MsrA (see Fig. 1 and see “Results and Discussion” under the paragraph “Rationale for the Substitutions”).

In view of this information, it was reasonable to postulate that Phe-52, Trp-53, His-186, Tyr-189, directly or indirectly, and Asp-129 and Tyr-197 residues are involved in the binding of the MetSO substrate via the ϵ -methyl group and the main chain, respectively. In the present study, all these residues of MsrA from *N. meningitidis* were substituted to validate their role. The catalytic parameters under steady-state conditions and of the reductase step of the mutated MsrAs were determined and compared with those of the wild type. Altogether, the results support the presence of at least two subsites involved in substrate binding. The first one, whose contribution is major, is the hydrophobic pocket formed by the side chains of invariant Phe-52 and Trp-53, the position of the latter being stabilized by interactions with His-186 and Tyr-189. The second subsite is composed of the side chains of invariant residues Asp-129 and Tyr-197.

EXPERIMENTAL PROCEDURES

Site-directed Mutagenesis, Production, and Purification of Mutated *N. meningitidis* MsrAs—The *E. coli* strain used for all *N. meningitidis* MsrA productions was BE002 (MG1655 msrA::specW, msrB::a3kana), transformed with plasmid pSKPILBMsrA containing only the coding sequence of MsrA from *pilB*, under the *lac* promoter (7). The BE002 strain was kindly provided by Dr F. Barras. Its use prevented expression of endogenous wild-type MsrA and MsrB from *E. coli*, and thus, avoided any contamination of the activity of the *N. meningitidis* MsrA by the Msrs from *E. coli*. Site-directed mutageneses were performed using the QuikChange site-directed mutagenesis kit (Stratagene).

Purifications were realized as described previously (11). Mutated MsrAs were pure, as verified by electrophoresis on a 12.5% SDS-PAGE gel followed by Coomassie Brilliant Blue R-250 staining and by electrospray mass spectrometry analyses.

Enzymes were stored as described previously. The molecular concentration was determined spectrophotometrically, using extinction coefficient at 280 nm of $26,200 \text{ M}^{-1}\cdot\text{cm}^{-1}$ for all mutated MsrAs except W53A and W53F MsrAs, which corresponded to an extinction coefficient of $20,480 \text{ M}^{-1}\cdot\text{cm}^{-1}$.

Steady-state MsrA Kinetics in the Presence of the Trx-recycling System—Steady-state kinetic parameters were determined with the Trx reductase recycling system (*E. coli* Trx reductase (1.2 μM), NADPH (0.3 mM)) with saturating concentration of *E. coli* Trx (100 μM) and by varying the concentrations of AcMetSONHMe. Initial rate measurements were carried out at 25 °C in buffer A (50 mM Tris-HCl, 2 mM EDTA, pH 8) on a Kontron Uvikon 933 spectrophotometer by following the decrease of the absorbance at 340 nm due to the oxidation of NADPH. Initial rate data were fit to the Michaelis-Menten relationship using least squares analysis to determine k_{cat} and K_m for AcMetSONHMe. *E. coli* Trx1 and Trx reductase were prepared following experimental procedures already published (19, 20). Ac-L-Met-R,S-SO-NHMe was prepared and purified as described previously (12).

Fluorescence Properties of Mutated MsrAs—The fluorescence excitation and emission spectra of mutated MsrAs, in their reduced and Cys-51/Cys-198 disulfide states, were recorded on an flx spectrofluorometer (SAFAS) thermostated at 25 °C in buffer A with 10 μM of each protein, as described previously (11). For the determination of λ_{max} of the emission spectrum and of the fluorescence intensity at λ_{max} , the excitation wavelength was 295 nm, and the emission was measured from 300 to 450 nm using a 10-nm band-pass for excitation and emission.

Determination of the Rate of AcMetNHMe Formation by Single Turnover Quenched-flow Experiments for W53F MsrA—Quenched-flow measurements were carried out at 25 °C on a SX18MV-R stopped-flow apparatus (Applied PhotoPhysics) fitted for double mixing and adapted to recover the quenched samples, as described previously (11). The apparatus operated in a pulsed mode. Under the conditions used, a minimum aging time of about 25–40 ms was determined. Equal volumes (57.5 μl) of a solution containing 550 μM of W53F MsrA in buffer A and a solution containing AcMetSONHMe in buffer A were mixed in the aging loop. The mixture was then allowed to react for the desired time before being mixed with 115 μl of a quenched aqueous solution containing 2% of trifluoroacetic acid. Quenched samples were collected in a 200- μl loop. For each aging time, four shots were done, and the four corresponding quenched samples were pooled in a volume of 700 μl and then analyzed.

After centrifugation, AcMetNHMe quantification in the resulting supernatant was carried out by reverse phase chromatography; 100 μl were injected onto a 4.6×250 -mm Atlantis dC18 reverse phase column (Waters) on an AKTA explorer system (Amersham Biosciences), equilibrated with $\text{H}_2\text{O}/0.1\%$ trifluoroacetic acid. AcMetNHMe was eluted after AcMetSONHMe, with a linear gradient of acetonitrile.

Data were plotted as mol of AcMetNHMe formed per mol of MsrA as a function of time. The rate of AcMetNHMe formation was determined by fitting the curve to the monoexponen-

Substrate Specificity of MsrA

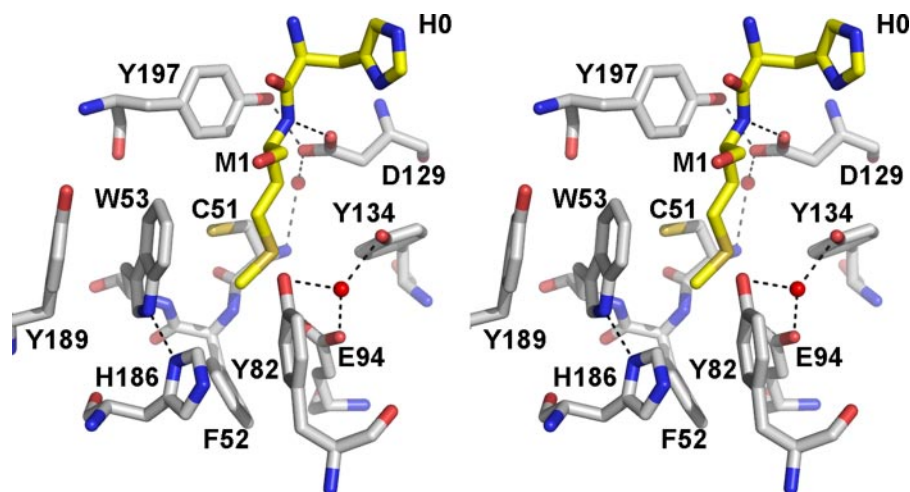


FIGURE 1. Stereo view of the *M. tuberculosis* MsrA active site containing Met-1 from a neighboring monomer (Protein Data Bank code 1NWA (17)). Residues Cys-51, Phe-52, Trp-53, Tyr-82, Glu-94, Tyr-134, His-186, Asp-129, Tyr-189, and Tyr-197 are shown in stick representation (carbon atoms in gray) together with bound His-0–Met-1 dipeptide from a neighboring monomer (carbon atoms in yellow). His-0 is part of the N-terminal His₁₀ tag used to obtain the recombinant *M. tuberculosis* MsrA. Phe-52, Trp-53, and Tyr-82 are located in α -helix, whereas Glu-94, Tyr-134, and Asp-129 belong to β -strands, and His-186, Tyr-189, and Tyr-197 are located in the C-terminal coil. Two water molecules are also represented by red spheres, and hydrogen bonds are shown as black dashed lines. The figure was generated using the program PyMOL (DeLano Scientific LLC).

tial Equation 1, in which a represents the fraction of AcMetNHMe formed per mol of MsrA and $k_{\text{AcMetNHMe}}$ the rate constant.

$$y = a(1 - e^{-k_{\text{AcMetNHMe}}t}) \quad (\text{Eq. 1})$$

Kinetics of the Formation of the Cys-51/Cys-198 MsrA Disulfide Bond in the Absence of Reductant by Single Turnover Stopped-flow Experiment at pH 8—Kinetics of the Trp-53 fluorescence variation associated with the formation of the Cys-51/Cys-198 disulfide bond were measured for F52L, D129A, D129N, H186A, H186N, Y189A, Y189F, Y197A, and Y197F MsrAs at 25 °C on a SX18MV-R stopped-flow apparatus (Applied PhotoPhysics) fitted for fluorescence measurements, as described previously (11). The excitation wavelength was set at 284 nm, and the emitted light was collected using a 320-nm cutoff filter. One syringe contained MsrA in buffer A (10 μM final concentration after mixing), and the other one contained AcMetSONHMe at various concentrations, *i.e.* up to 200 mM for Y197A and Y197F MsrAs and up to 800 mM for F52L, D129A, D129N, H186A, H186N, Y189A, and Y189F MsrAs in buffer A. An average of at least six runs was recorded for each AcMetSONHMe concentration. Rate constants, k_{obs} , were obtained by fitting fluorescence traces with the monoexponential Equation 2, in which c represents the end point and a represents the amplitude of the fluorescence increase (<0). For all mutated MsrAs, the variation of the fluorescence signal as a function of time was of monoexponential type irrespective of the substrate concentration used.

$$y = ae^{-k_{\text{obs}}t} + c \quad (\text{Eq. 2})$$

When saturating concentrations of AcMetSONHMe were observed (for H186N and Y189F MsrAs), the data were fit to Equation 3 using least square analysis to determine $k_{\text{obs max}}$ and

K_S for AcMetSONHMe. S represents the AcMetSONHMe concentration and K_S the apparent affinity constant.

$$k_{\text{obs}} = \frac{k_{\text{obs max}}S}{K_S + S} \quad (\text{Eq. 3})$$

To determine the pseudo-second-order constant (k_2) values, subsaturating concentrations of AcMetSONHMe were used, from 1 to 50 mM for F52L, D129A, D129N, H186A, H186N, Y189A, Y197A, and Y197F MsrAs and from 1 to 20 mM for wild-type and Y189F MsrAs. The slope (k_2) of the rate constant (k_{obs}) plotted against the substrate concentration was obtained by linear fitting. For D129A, D129N, Y197A, Y197F, and wild-type MsrAs, k_2 values were also determined with subsaturating concentrations of L-Met-*R,S*-SO and dimethyl sulfoxide as a substrate.

RESULTS AND DISCUSSION

Rationale for the Substitutions

As indicated in the Introduction, invariant Phe-52 and Trp-53 form a hydrophobic pocket in which one of the methyl groups of dimethyl arsenate in *E. coli* MsrA and the ϵ -methyl group of Met-1 in *M. tuberculosis* MsrA is bound (Fig. 1). Therefore, this strongly supported binding of the ϵ -methyl group of MetSO to this pocket. Inspection of the MsrA active sites also shows the existence of (i) a hydrogen bond between the NH group of the Trp-53 indole ring and the N δ of His-186 (distance of 2.9 Å) and (ii) a stacking of the Trp-53 indole ring with the phenyl ring of Tyr-189, the two aromatic rings being parallel at 3.4 Å from each other. These interactions are likely essential to stabilize the positioning of the indole ring adequate for efficient binding of the MetSO substrate via its ϵ -methyl group. Thus, two types of substitutions were performed: 1) those that are expected to significantly perturb the binding of the ϵ -methyl of the substrate, either directly (F52L,⁴ W53A, and W53F MsrAs) or indirectly (H186A and Y189A MsrAs), and thus, can lead to a K_S and a $k_{\text{obs max}}$ effects; and 2) those that conserve the ability to position efficiently the indole ring of Trp-53 (H186N by hydrogen bond via the amide function and Y189F by stacking via the phenyl ring) and therefore are expected to have little effect on the kinetic parameters of the reductase step.

As mentioned in the Introduction, Asp-129 and Tyr-197 were postulated to stabilize the main chain of the substrate. Indeed, the inspection of the *M. tuberculosis* MsrA active site, which is occupied by the Met-1 residue, shows that the carboxylate group of Asp-129 makes two hydrogen bonds: 1) one with

⁴ For unknown reasons, it was not possible to produce F52V and F52A MsrAs.

the NH α of Met-1 engaged in a peptidic bond with His-0 and 2) the other with the hydroxyl group of Tyr-197. Moreover, the Tyr-197 phenyl ring also forms a stacking interaction with the peptide bond between His-0 and Met-1. Thus, to determine their role, Asp-129 and Tyr-197 residues were both substituted: 1) by Ala to disrupt all the stabilizing interactions that can exist and 2) by Asn and Phe, respectively, to conserve one putative stabilizing interaction.

Justification of the Methods Used to Characterize the Properties of the Mutated MsrAs

As indicated in the Introduction, the rate of the reductase step in MsrA is fast and largely higher than the k_{cat} value. Therefore, to interpret the consequences of a substitution on the kinetic parameters of the reductase step, it was necessary to attain the rate of the reductase step for each mutated MsrA. For that, we took advantage of the Trp-53 fluorescence emission signal intensity of all the mutated MsrAs, except for W53F MsrA, which varied from the reduced to the oxidized disulfide form. In fact, formation of the disulfide bond led to an increase in the Trp-53 fluorescence emission for D129A, D129N, H186N, Y189F, Y197A, and Y197F MsrAs similarly to that described for the wild type (11), whereas a quenching was observed for F52L, H186A, and Y189A MsrAs, which is due to an increase of the fluorescence intensity of the reduced form of these mutated MsrAs (see below, paragraph "Fluorescence Properties of F52L, H186A/H186N, and Y189A/Y189F MsrAs"). For all mutated MsrAs, the rate of the reductase step was determined under single turnover conditions, *i.e.* in the absence of reductant as already described for the wild type (11). In that context, we have assumed that the reductase step was still rate-determining in the process, leading to formation of the Msr disulfide bond, as demonstrated previously for the wild type (11). For all mutated MsrAs, k_2 values that are representative of the $k_{\text{obs max}}/K_S$ values were determined under subsaturating concentrations of AcMetSONHMe. When saturating concentration of AcMetSONHMe was observed, K_S and $k_{\text{obs max}}$ values were also determined.

In the absence of the fluorescent probe Trp-53, the kinetics of the reductase step for the W53F MsrA was attained by following the rate of formation of AcMetNHMe under single turnover conditions, *i.e.* in the absence of reductant (11). This was done only at two concentrations of AcMetSONHMe (300 and 600 mM) with the use of a rapid mixing apparatus. Formation of ~ 0.9 mol of AcMetNHMe/mol of W53F MsrA was observed for both substrate concentrations.

The kinetic experiments were performed with AcMetSONHMe as a substrate for all mutated MsrAs. The rationale is that the wild-type MsrA was previously shown to exhibit a better affinity for AcMetSONHMe (K_S value of 55 mM) when compared with MetSO, *i.e.* by a factor of at least 20, in the reductase step (9, 11). Thus, AcMetSONHMe can be considered as a better mimic of MetSO included in proteins when compared with free MetSO. For mutated MsrAs at positions 129 and 197, k_2 values were determined not only with AcMetSONHMe but also with MetSO and Me₂SO. Indeed, comparison of the k_2 values can provide information

TABLE 1
Steady-state and reductase step kinetic parameters of wild-type and mutated MsrAs

Steady-state parameters were deduced from nonlinear regression of initial rates to the Michaelis-Menten relationship. k_2 values of the reductase step were obtained by linear regression of k_{obs} determined under subsaturating concentration of substrate (see "Experimental Procedures"). It is important to note that the K_m values have to be divided by 2 and the k_2 values have to be multiplied by 2, taking into account the fact that the *R* isomer of the sulfoxide function is neither a substrate nor an inhibitor of MsrA (7). ND, not determined.

Enzyme	Steady-state		Reductase step ($k_{2 \text{ AcMetSONHMe}}$)
	k_{cat}	K_m AcMetSONHMe	
	s^{-1}	<i>mM</i>	$mM^{-1} \cdot s^{-1}$
Wild type	3.4 \pm 0.2	0.6 \pm 0.2	14.9 \pm 0.9
F52L	0.5 \pm 0.1	39 \pm 8	0.02 \pm 0.01
W53A	0.3 \pm 0.1	800 \pm 300	ND
W53F	0.8 \pm 0.1	36 \pm 1	0.015 ^a
H186A	2.6 \pm 0.3	99 \pm 1	0.12 \pm 0.01
H186N	3.1 \pm 0.3	2.6 \pm 0.9	4.5 \pm 0.1
Y189A	2.5 \pm 0.2	34 \pm 9	0.60 \pm 0.02
Y189F	1.8 \pm 0.1	0.3 \pm 0.1	13.0 \pm 0.5
D129A	1.7 \pm 0.3	10 \pm 4	0.40 \pm 0.01
D129N	1.8 \pm 0.1	6 \pm 1	0.80 \pm 0.01
Y197A	1.3 \pm 0.1	1.5 \pm 0.3	1.90 \pm 0.04
Y197F	3.5 \pm 0.3	3 \pm 1	4.8 \pm 0.3

^a The k_2 value was an estimation obtained from only two substrate concentrations (300 and 600 mM, see "Results," paragraph "Kinetic Properties of F52L and W53F/W53A MsrAs").

on the structural factors that are responsible for the enhanced affinity of MsrA for AcMetSONHMe.

Characterization of the amino acids involved in the recognition of the ϵ -methyl group of Ac-L-MetSONHMe

Kinetic Properties of F52L and W53F/W53A MsrAs—As shown in Table 1, the substitution of Phe-52 by Leu and Trp-53 by Phe or Ala resulted in a significant increase of the K_m value for AcMetSONHMe from 60- to 1300-fold, whereas the k_{cat} value decreased in the range of only 4–11-fold. Under single turnover conditions, no saturating kinetic effects with respect to AcMetSONHMe were observed for F52L MsrA up to 800 mM substrate (Fig. 2A). The k_{obs} value determined at 800 mM substrate was 16-fold higher than the k_{cat} value for F52L MsrA, indicating a rate-limiting step still associated with the Trx-recycling step. The k_2 value of 0.02 $mM^{-1} \cdot s^{-1}$ decreased 745-fold when compared with that of the wild type. For W53F MsrA, k_{obs} values of 5.2 and 8.5 s^{-1} for AcMetNHMe formation were determined at 300 and 600 mM AcMetSONHMe, respectively (Fig. 3). These data indicated: 1) a rate-limiting step still associated with the Trx-recycling step and 2) a substrate saturating effect not yet attained at 600 mM AcMetSONHMe. A k_2 value of ~ 0.015 $mM^{-1} \cdot s^{-1}$ can be estimated that is ~ 1000 -fold smaller than the k_2 value of the wild type (Table 1). For both W53F and F52L MsrAs, the k_{obs} value at a substrate concentration of 600 and 800 mM, respectively, is at least 80-fold lower than the $k_{\text{obs max}}$ of the wild type. Therefore, the 750–1000-fold decrease in k_2 reflects both a $k_{\text{obs max}}$ effect and a K_S effect. Therefore, it is probable that substituting Phe for Trp-53 and Leu for Phe-52 disrupts, in part, the hydrophobic pocket, and as a consequence, not only decreases the affinity of the substrate by a factor that can be estimated to be at least 20 but also perturbs the positioning of the sulfoxide function relative to that of the catalytic amino acids involved in the sulfoxide reduction. The situation is probably the same and even more pronounced

Substrate Specificity of MsrA

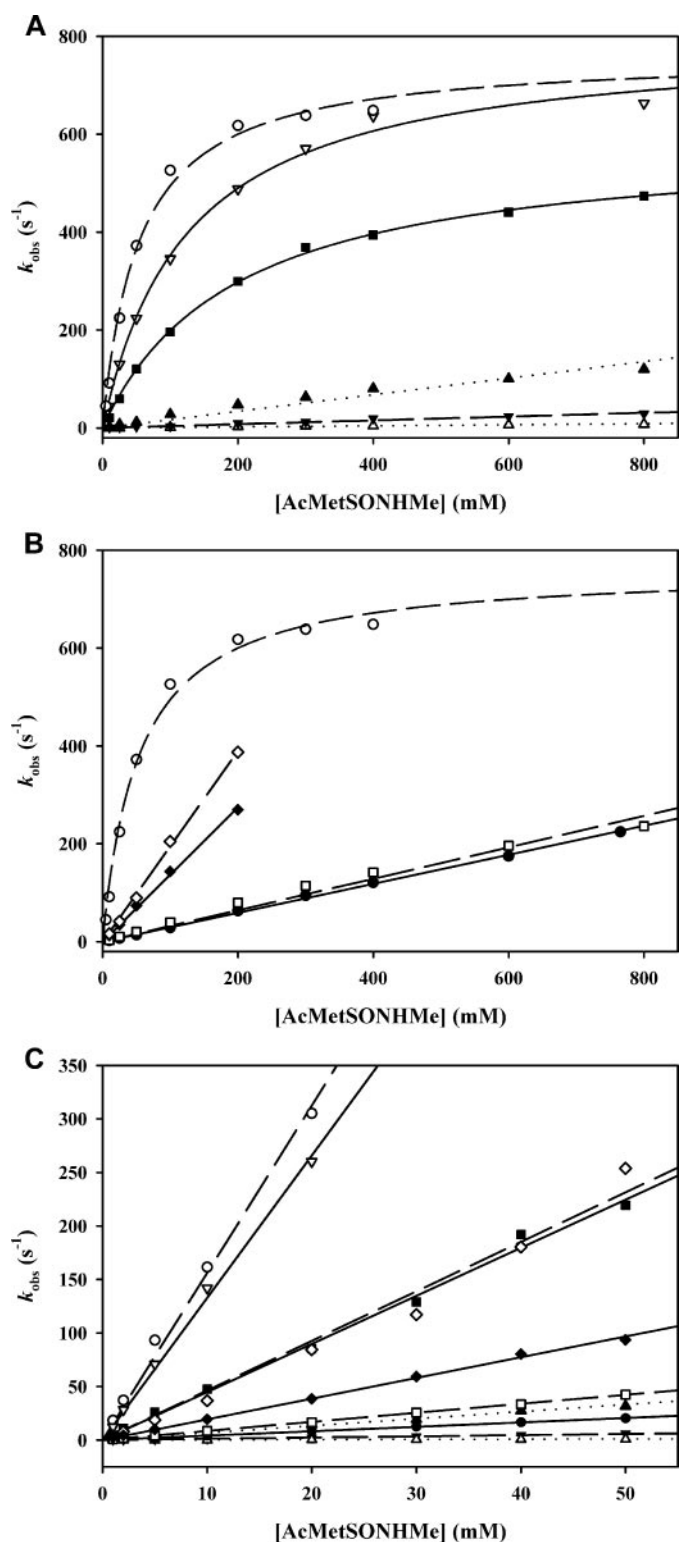


FIGURE 2. Determination of the catalytic parameters of the reductase step of wild-type, F52L, H186A/H186N, Y189A/Y189F, D129A/D129N, and Y197A/Y197F MsrAs measured by fluorescence stopped-flow under single turnover kinetics. The MsrA fluorescence variation was recorded on a stopped-flow apparatus at 25 °C. Final concentration of MsrA was 10 μM . Excitation wavelength was set at 284 nm, and emitted light was collected above 320 nm using a cut-off filter. For each substrate concentration, experimental data were analyzed by nonlinear regression against Equation 2 to obtain k_{obs} . In A and B, the substrate range was from 10 to 800 mM. For H186N and Y189F MsrAs, saturating concentrations of AcMetSONHMe were observed, and k_{obs} data were fit to Equation 3, which gave $k_{\text{obs max}}$ and K_S values as follows: Y189F

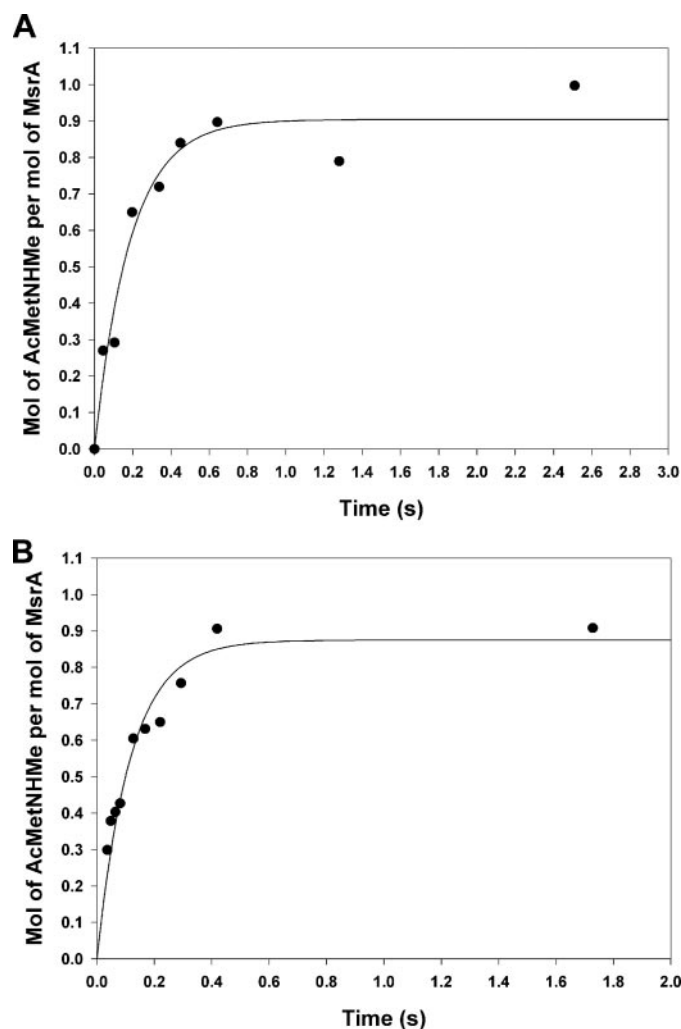


FIGURE 3. Time-resolved appearance of Ac-L-Met-NHMe for the W53F MsrA under single turnover kinetics. The quenched-flow experiments were carried out at 25 °C in 50 mM Tris-HCl, pH 8, at 300 (A) and 600 mM (B) of AcMetSONHMe as described under "Experimental Procedures." The symbols represent experimental data points. Data were fit to Equation 1 and gave rate constants of 5.2 ± 1.0 and $8.5 \pm 1.0 \text{ s}^{-1}$ with amplitudes of 0.90 ± 0.05 mol of Ac-L-Met-NHMe/mol of enzyme and 0.87 ± 0.04 mol of Ac-L-Met-NHMe/mol of enzyme in the presence of 300 and 600 mM substrate, respectively.

when Trp-53 is substituted by Ala, as suggested by the very high K_m value for the substrate (800 mM when compared with 0.6 mM for the wild type).

Kinetic Properties of H186A/H186N and Y189A/Y189F Msrs—The kinetic constants determined for the H186A, H186N,

MsrA (A, ∇ , solid line, $k_{\text{obs max}} = 800 \pm 30 \text{ s}^{-1}$ and $K_S = 130 \pm 10 \text{ mM}$); H186N MsrA (A, \blacksquare , solid line, $k_{\text{obs max}} = 590 \pm 10 \text{ s}^{-1}$ and $K_S = 200 \pm 10 \text{ mM}$). For F52L, H186A, Y189A, D129A/D129N, and Y197A/Y197F Msrs, no saturating concentrations of AcMetSONHMe were observed, and k_{obs} data were fit to the linear equation as follows: F52L MsrA (A, \triangle , dotted line); H186A MsrA (A, ∇ , dashed line); Y189A MsrA (A, \blacktriangle , dotted line); D129A MsrA (B, \bullet , solid line); D129N (B, \square , dashed line); Y197A MsrA (B, \blacklozenge , solid line); Y197F MsrA (B, \diamond , dashed line). The symbols represent data, and the lines represent the fit. The data of the wild-type MsrA were also presented as reference (A and B, \circ , dashed line, $k_{\text{obs max}} = 790 \pm 10 \text{ s}^{-1}$ and $K_S = 55 \pm 2 \text{ mM}$ (9)). In C, the substrate range was from 1 to 50 mM. The k_2 values were obtained by linear fitting of k_{obs} values for wild-type (\circ , dashed line), F52L (\triangle , dotted line), D129A (\bullet , solid line), D129N (\square , dashed line), H186A (∇ , dashed line), H186N (\blacksquare , solid line), Y189A (\blacktriangle , dotted line), Y189F (∇ , solid line), Y197A (\blacklozenge , solid line), and Y197F (\diamond , dashed line) Msrs.

Y189A, and Y189F MsrAs under steady-state conditions showed that the k_{cat} is not modified for all mutated MsrAs (Table 1). The K_m values varied slightly for the H186N and Y189F MsrAs (4-fold increase and 2-fold decrease, respectively) but were strongly increased for the H186A and Y189A MsrAs (165- and 57-fold, respectively) when compared with that of the wild type.

Under single turnover conditions, a saturating kinetics effect with respect to AcMetSONHMe concentration was only observed for H186N and Y189F MsrAs, whereas no saturating effect was observed for H186A and Y189A MsrAs up to 800 mM (Fig. 2, A and B). The k_{obs} values determined at 800 mM substrate were 11-, 52-, 190-, and 444-fold higher than the k_{cat} values for H186A, Y189A, H186N, and Y189F MsrAs, respectively, indicating a rate-limiting step still associated with the Trx-recycling step. The K_S , $k_{\text{obs max}}$, and k_2 values determined for H186N and Y189F MsrAs were in the range of those determined for the wild type (Fig. 2B and Table 1). This was not the case when His-186 or Tyr-189 was substituted by Ala, as probed by the 124- and 25-fold k_2 decrease observed, respectively. The k_2 decreases reflect both a K_S effect and a $k_{\text{obs max}}$ effect since the k_{obs} values determined at 800 mM AcMetSONHMe were decreased by 27- and 6-fold for H186A and Y189A MsrAs, respectively, when compared with the $k_{\text{obs max}}$ value of the wild type. When compared with the W53F MsrA, the k_2 values for H186A and Y189A are decreased less. Altogether, the kinetic data are thus in accord with the postulated role of His-186 and Tyr-189 that favored an efficient positioning of the Trp-53 indole ring via a hydrogen bond and a stacking interaction, respectively. This also agrees with the fact that the conservative substitutions of His-186 and Tyr-189 by Asn and Phe, respectively, have no significant effect on the catalytic efficiency of the reductase step.

Fluorescence Properties of F52L, H186A/H186N, and Y189A/Y189F MsrAs—Previous work showed that the fluorescence properties of wild-type MsrA, when excitation was performed at 295 nm, were only due to the contribution of Trp-53 and consequently reflect the microenvironment of the Trp-53 indole ring (11). Comparison of the emission spectra of all mutated MsrAs with that of the wild-type, of either the reduced or the oxidized disulfide forms, showed no difference except for the reduced form of F52L, H186A, and Y189A MsrAs (spectra not shown). For these mutated MsrAs, the λ_{max} is shifted from 338 to 346 nm, which reflects a microenvironment of the indole side chains of Trp-53 more polar than in the reduced forms of the wild type and the other mutated MsrAs. This is likely due to an increased accessibility of Trp-53 to solvent. Moreover, in contrast to other mutated MsrAs, in particular to H186N and Y189F MsrAs, F52L, H186A, and Y189A MsrAs display a 3.8-, 2.3-, and 2.7-fold increase of the fluorescence intensity at λ_{max} , respectively, when compared with that of the wild type (spectra not shown). This reflects a lesser quenching of the Trp-53 fluorescence. As already mentioned, inspection of the x-ray MsrA structure shows a π - π stacking interaction between the phenyl ring of Tyr-189 and the indole ring of Trp-53. Therefore, Tyr-189 is a good candidate as the quencher of the Trp-53 fluorescence in the wild type. This is in accord with the increase of the Trp-53 fluorescence intensity, which is observed in Y189A

MsrA but not in Y189F MsrA that still possesses a phenyl ring. The increase of the fluorescence intensity observed for H186A MsrA and F52L MsrA suggests a separation taking place between Trp-53 and the phenyl ring of Tyr-189 in both mutated MsrAs. In both cases, it is probable that the positioning of the indole ring relative to that of Tyr-189 is perturbed. For H186A, it is likely the consequence of the loss of a hydrogen bond with the indole ring of Trp-53. As a support, H186N MsrA, which conserves the capacity of forming a hydrogen bond, displays similar λ_{max} and fluorescence intensity as the wild type. In the case of F52L, it is probable that substituting Leu for Phe-52 disrupts, in part, the hydrophobic pocket, and in return, destabilizes the positioning of Trp-53 relative to Tyr-189. These interpretations are in accord with the K_S effects observed for F52L, H186A, and Y189A MsrAs.

Role of Asp-129 and Tyr-197 in the recognition of the main chain of the substrate

The kinetic parameters of D129A, D129N, Y197A, and Y197F MsrAs determined under steady-state conditions showed that the k_{cat} value was not modified, whereas the K_m value was increased 16-, 10-, 2.5-, and 5-fold, respectively, when compared with those of the wild type (Table 1). Under single turnover conditions in the absence of reductant, no kinetic saturation effect was observed up to 800 and 200 mM AcMetSONHMe for D129A/D129N and Y197A/Y197F⁵ MsrAs, respectively (Fig. 2C). The k_{obs} values determined at substrate concentration of 800 mM for D129A and D129N MsrAs and of 200 mM for Y197A and Y197F MsrAs were 141-, 133-, 208-, and 110-fold higher than their corresponding k_{cat} values, indicating a rate-limiting step still associated with the Trx-recycling step for all these mutated MsrAs.

The k_2 values were 37-, 19-, 8-, and 3-fold decreased for D129A, D129N, Y197A, and Y197F MsrAs, respectively, when compared with that of the wild type (Table 1). These decreases in k_2 reflect essentially a K_S effect since the k_{obs} values determined at 800 and 200 mM AcMetSONHMe decreased only 2–3-fold for D129A/D129N and Y197A/Y197F MsrAs, respectively, when compared with the $k_{\text{obs max}}$ value of the wild type.

The fact that Asp-129 and Tyr-197 were predicted from the three-dimensional structure of MsrA from *M. tuberculosis* complexed with a Met residue to stabilize the main chain of the substrate raised the question whether they can discriminate in favor of the binding of a protein-bound MetSO against the binding of free MetSO. Indeed, MsrA displays a better affinity of at least 20-fold for AcMetSONHMe when compared with free MetSO. As shown in Table 2, substituting Asp-129 by Ala or Asn and Tyr-197 by Ala or Phe also affected the k_2 values with MetSO as a substrate with the same magnitude as with AcMetSONHMe, in contrast to Me₂SO, for which the k_2 values are not significantly modified except for D129A MsrA. Altogether, the data support: 1) a nondiscriminating role of Asp-129 and Tyr-197 in the recognition of the NH main chain of the MetSO with the amino and carboxyl groups of MetSO either

⁵ For Y197A/Y197F MsrAs, the variation of the fluorescence signal as a function of time becomes, for an unknown reason, not significant for substrate concentration higher than 200 mM.

TABLE 2

Reductase step second order rate constants k_2 of wild-type and mutated MsrAs with different sulfoxide substrates

k_2 values of the reductase step were obtained by linear regression of k_{obs} determined under subsaturating concentration of substrate (see "Experimental Procedures"). The number in brackets represents the k_2 value of mutated MsrAs when compared with the k_2 value of the wild type expressed in percentage. It is important to note that the k_2 constant for Ac-L-Met-R,S-SO-NHMe and for L-Met-R,S-SO, in contrast to the k_2 constant for Me₂SO, have to be multiplied by 2, taking into account the fact that the R isomer of the sulfoxide function is neither a substrate nor an inhibitor of MsrA (7).

Enzyme	k_2 AcMetSONHMe	k_2 MetSO $mm^{-1}s^{-1}$	k_2 Me ₂ SO
Wild type	14.9 ± 0.9 (100)	1.40 ± 0.01 (100)	0.50 ± 0.01 (100)
D129A	0.40 ± 0.01 (2.7)	0.03 ± 0.01 (2)	0.18 ± 0.01 (36)
D129N	0.80 ± 0.01 (5.4)	0.12 ± 0.01 (9)	0.42 ± 0.01 (84)
Y197A	1.90 ± 0.04 (13)	0.40 ± 0.01 (29)	0.36 ± 0.01 (72)
Y197F	4.8 ± 0.3 (32)	0.50 ± 0.01 (36)	0.30 ± 0.01 (60)

free, and thus, charged, or engaged in amide bonds, as is the case for a protein-bound MetSO; and 2) a higher contribution of Asp-129 to the substrate binding when compared with Tyr-197. Nevertheless, the fact that a phenyl ring can make interaction with a peptidic bond as well as with a protonated amine (21, 22) prevents discrimination between a direct role of Tyr-197 in substrate binding or an indirect role, via the orientation of the carboxylate group of Asp-129. Anyway, the contribution of Asp-129 and Tyr-197 remains modest when compared with that of Phe-52 and Trp-53 in terms of K_S values.

The selectivity of MsrA for protein-bound MetSO should thus arise from other structural factors (either a stabilizing effect for protein-bound MetSO via interactions with the amide bonds or a destabilizing effect for MetSO due to repulsive interactions with the charges on the amino and/or carboxyl groups) located near the active site of the MsrA. These factors, if existing, remain to be characterized. In that context, determination of the three-dimensional structure of a complex between a MsrA and a protein MetSO substrate could provide additional information to those obtained from the three-dimensional structure of MsrA from *M. tuberculosis* complexed with a Met residue.

Conclusion

We have shown that for MsrA: 1) the hydrophobic pocket, formed by the side chains of invariant Phe-52 and Trp-53, is the major factor that contributes to MetSO binding via interactions with the ϵ -methyl group; 2) invariant His-186 and Tyr-189 are key residues for orienting the Trp-53 indole ring, the positioning of which is essential for an efficient reductase activity to occur; and 3) the side chains of invariant residues Asp-129 and Tyr-197 participate in the substrate binding but are not discriminating in terms of binding between a MetSO either engaged in amide bonds or with amino and carboxyl groups free. The K_f value of MsrA for AcMetNHMe is at least 2 M (data not shown). This shows a low affinity of MsrA for AcMetNHMe, although the ϵ -methyl group is present. As indicated in the Introduction, Glu-94, Tyr-82, and Tyr-134 are involved in catalysis but not in substrate binding. Moreover, a MetSO substrate such as AcMetSONHMe is bound to the active site with its sulfoxide function largely polarized via interactions with Glu-94, Tyr-82, and Tyr-134. Therefore, the sulfur of the sulfoxide function bears a positive charge, or at least a partial charge, and thus,

participates by a substrate-assisted mechanism to interacting and stabilizing the thiolate form of Cys-51 (14). In contrast, the sulfur of AcMetNHMe is rather negatively charged (23, 24). Thus, a repulsive electrostatic interaction is expected to occur between the sulfur of Cys-51 and the sulfur of the product, which can be considered as an anti-determinant factor that disfavors binding of product such as AcMetNHMe. The consequence is either a higher rate of dissociation of the product from the MsrA-product complex when compared with that of a MsrA-MetSO complex and/or a lower rate of association of the product to MsrA when compared with that of MetSO substrate, and thus, would explain the low affinity of MsrA for AcMetNHMe.

Recent structural and dynamical NMR studies of both reduced and oxidized forms of *E. coli* MsrA (25) show the existence of a conformational switch that would be a prerequisite to form the Cys-51/Cys-198 bond. The consequence is a solvent exposition of the hydrophobic surface of the active site of the oxidized MsrA, which could permit an efficient interaction with Trx. The switch only concerns two segments that contain Asp-129 and Tyr-197 residues, respectively. In the oxidized form, the distance between Asp-129 and Tyr-197 is too large for hydrogen bond interaction between both residues in contrast to what is observed in reduced form. It is probable that the release of the product for which MsrA displays low affinity is the driving factor responsible for the conformational switch.

Acknowledgments—We thank Dr. F. Barras for the kind gift of the BE002 *E. coli* strain, C. Gauthier for the AcMetSONHMe synthesis, Dr. G. Chevreux and Dr. S. Sanglier-Cianferani for mass spectrometry analyses, Dr. G. Monard for helpful discussion, and Dr. S. Sonkaria for the careful reading of the manuscript.

REFERENCES

- Vogt, W. (1995) *Free Radic. Biol. Med.* **18**, 93–105
- Schoneich, C. (2005) *Biochim. Biophys. Acta* **1703**, 111–119
- Moskovitz, J. (2005) *Biochim. Biophys. Acta* **1703**, 213–219
- Weissbach, H., Resnick, L., and Brot, N. (2005) *Biochim. Biophys. Acta* **1703**, 203–212
- Ezraty, B., Aussel, L., and Barras, F. (2005) *Biochim. Biophys. Acta* **1703**, 221–229
- Boschi-Muller, S., Azza, S., Sanglier-Cianferani, S., Talfournier, F., Van Dorsselear, A., and Branlant, G. (2000) *J. Biol. Chem.* **275**, 35908–35913
- Olry, A., Boschi-Muller, S., Marraud, M., Sanglier-Cianferani, S., Van Dorsselear, A., and Branlant, G. (2002) *J. Biol. Chem.* **277**, 12016–12022
- Neiers, F., Kriznik, A., Boschi-Muller, S., and Branlant, G. (2004) *J. Biol. Chem.* **279**, 42462–42468
- Boschi-Muller, S., Olry, A., Antoine, M., and Branlant, G. (2005) *Biochim. Biophys. Acta* **1703**, 231–238
- Boschi-Muller, S., Azza, S., and Branlant, G. (2001) *Protein Sci.* **10**, 2272–2279
- Antoine, M., Boschi-Muller, S., and Branlant, G. (2003) *J. Biol. Chem.* **278**, 45352–45357
- Olry, A., Boschi-Muller, S., and Branlant, G. (2004) *Biochemistry* **43**, 11616–11622
- Balta, B., Monard, G., Ruiz-Lopez, M. F., Antoine, M., Gand, A., Boschi-Muller, S., and Branlant, G. (2006) *J. Phys. Chem. A* **110**, 7628–7636
- Antoine, M., Gand, A., Boschi-Muller, S., and Branlant, G. (2006) *J. Biol. Chem.* **281**, 39062–39070
- Tete-Favier, F., Cobessi, D., Boschi-Muller, S., Azza, S., Branlant, G., and Aubry, A. (2000) *Structure Fold. Des.* **8**, 1167–1178

16. Lowther, W. T., Brot, N., Weissbach, H., and Matthews, B. W. (2000) *Biochemistry* **39**, 13307–13312
17. Taylor, A. B., Benglis, D. M., Jr., Dhandayuthapani, S., and Hart, P. J. (2003) *J. Bacteriol.* **185**, 4119–4126
18. Rouhier, N., Kauffmann, B., Tete-Favier, F., Paladino, P., Gans, P., Branlant, G., Jacquot, J. P., and Boschi-Muller, S. (2007) *J. Biol. Chem.* **282**, 3367–3378
19. Mulrooney, S. B. (1997) *Protein Expression Purif.* **9**, 372–378
20. Mossner, E., Huber-Wunderlich, M., and Glockshuber, R. (1998) *Protein Sci.* **7**, 1233–1244
21. Gruez, A., Roig-Zamboni, V., Grisel, S., Salomoni, A., Valencia, C., Campanacci, V., Tegoni, M., and Cambillau, C. (2004) *J. Mol. Biol.* **343**, 29–41
22. Tsou, L. K., Tatko, C. D., and Waters, M. L. (2002) *J. Am. Chem. Soc.* **124**, 14917–14921
23. Chipot, C., Angyan, J. G., Maigret, B., and Scheraga, H. A. (1993) *J. Phys. Chem.* **97**, 9788–9796
24. Guillot, R., Muzet, N., Dahaoui, S., Lecomte, C., and Jelsch, C. (2001) *Acta Crystallogr. Sect. B Struct. Crystallogr.* **57**, 567–578
25. Coudeville, N., Antoine, M., Bouguet-Bonnet, S., Mutzenhardt, P., Boschi-Muller, S., Branlant, G., and Cung, M. T. (2007) *J. Mol. Biol.* **366**, 193–206

**Characterization of the Amino Acids Involved in Substrate Specificity of
Methionine Sulfoxide Reductase A**

Adeline Gand, Mathias Antoine, Sandrine Boschi-Muller and Guy Branlant

J. Biol. Chem. 2007, 282:20484-20491.

doi: 10.1074/jbc.M702350200 originally published online May 11, 2007

Access the most updated version of this article at doi: [10.1074/jbc.M702350200](https://doi.org/10.1074/jbc.M702350200)

Alerts:

- [When this article is cited](#)
- [When a correction for this article is posted](#)

[Click here](#) to choose from all of JBC's e-mail alerts

This article cites 25 references, 7 of which can be accessed free at
<http://www.jbc.org/content/282/28/20484.full.html#ref-list-1>